JOURNAL OF MATERIALS SCIENCE 25 (1990) 4495–4500

Microstructural and textural characterization of a commercial aluminium–lithium alloy

S. WISMAYER, B. RALPH
Department of Materials Technology, Brunel, The University of West London, Uxbridge, Middlesex UB8 2PH, UK

A chemical and textural investigation into the grain-banding effect found through 1.6 mm gauge aluminium–lithium aerospace sheet is presented. Wavelength dispersive X-ray spectroscopy was used to measure the copper content profile through the sheet whilst laser-induced ion mass analysis was used to establish the lithium profile. The pole figures derived by X-ray goniometric analysis are given at 400, 530 and 800 μm through the sheet, together with pole figures, collected via the electron backscattering technique. Both illustrate the textural data of grains at the surface and centre of the alloy sheet.

1. Introduction

The current aluminium–lithium commercialization programme was established to produce an aerospace alloy, with the same (or better) fracture toughness and strength as the conventional aluminium alloys, but with a reduced density. By doing so the lift-induced drag experienced by an aircraft would be reduced, so saving fuel [1]. Presently there are three categories of aluminium–lithium alloys under development designed to replace the current series: (a) damage tolerant (cf. 2024-T3); (b) medium strength (cf. 2014-T6 and 2475-T73); and (c) high strength (cf. 7075-T6) [2]. It is hoped that not only will a 10% reduction in density be achieved, and a 10% increase in stiffness, but standard engineering properties associated with the conventional alloys will be maintained [3]. It should be stressed that the use of a material with low fracture toughness should not be made, as cracks of nearly critical length may then be too small to detect [4].

It is an objective to be able to define a process for the production of an aluminium–lithium alloy to achieve a fracture toughness which is commercially acceptable, without deterioration of its other mechanical properties. By microstructural and textural characterization, it is hoped to determine the factors which control the microstructure and particularly the configuration of grain boundaries, under the driving forces of recrystallization and grain growth. Many investigators are presently working in this field, (e.g. [5]). As the low, short transverse ductility appears to arise from the overall array of planar grains (resulting in turn from the difficulty of recrystallizing aluminium alloys containing additions of lithium and zirconium [6]), the present study has been directed at an examination of the distribution of alloying constituents in the short transverse direction, and their possible effect upon grain morphology and texture. The concern here is with the specific elemental additions which are made to improve mechanical properties, but in so doing alter other equilibrium balances within the system. For example, zirconium is added to Al–Li alloys (and other aluminium alloys) because coherent Al_3Zr (β'), inhibits recrystallization [7]. However, the distribution of metastable coherent Al_3Zr (β') acts as preferential nucleation sites for the precipitation of Al_3Li (δ') – a major strengthening phase in Al–Li alloys [8, 9]. Also by preventing recrystallization, more highly textured structures are favoured, with the majority of grain boundaries being of the low-angle type. This influences other microstructural factors, including the precipitation of the AlLi (δ) phase, which preferentially nucleates and grows on high-angle boundaries [9]. The δ precipitation causes brittle grain-boundary fracture [9] and thus restricting recrystallization can improve the toughness. The whole process of precipitation hardening in lithium-containing alloys is complex. Not only is the formation of a large volume fraction of a metastable ordered and coherent Al_3Li (δ') phase involved [10, 11], but with copper present, additional strengthening is achieved by the co-precipitation of copper-rich phases, e.g. Al_2Cu (θ') independently of δ' [12]. In addition the interaction of aluminium, copper and lithium can result in the formation of Al_2CuLi [T_1'], which when present alongside the δ' phase is associated with a reduction in both strength and ductility [13].

Notwithstanding the chemical implications, strength and ductility are closely related to the characteristic behaviour of dislocations [14]. Because a microstructure which results in a good proof strength, is deleterious to fatigue toughness and stress corrosion resistance [15], refining the grain size remains the only way to increase both the strength and toughness; solution heat treating and precipitate hardening may decrease toughness considerably.

It was apparent that the desired increase in fracture toughness would be the result of a change to the thermomechanical process and/or a subtle alteration to the chemical make-up of the alloy sheet.

0022–2461/90 $03.00 + .12

TABLE I

Element	wt %
Li	2.32
Cu	1.10
Mg	0.82
Zr	0.07
Fe	0.09
Si	0.04
Ti	0.04

The as-received alloy was in the T3 condition. Further treatments given were: (i) solution heat treatment for 0.5 h at 540° C; (ii) age 16 h at 190° C. After each heat treatment the alloy was water quenched.

2. Experimental procedure

Our study concerned an aluminium–lithium alloy in sheet form with a composition given in Table I. The alloy was etched using Kellers reagent to reveal the grain structure.

The following techniques were employed: wavelength dispersive X-ray spectroscopy (WDS) in a scanning electron microscope; laser-induced ion mass analysis (LIMA); texture determination using: (1) an X-ray texture goniometer; (2) the electron back scattering (EBS) equipment in a scanning electron microscope.

2.1. Wavelength dispersive X-ray spectroscopy

Associated with a scanning electron microscope, this is a highly accurate technique for the identification and quantification of a great number of elements, more so than energy dispersive X-ray spectroscopy (e.g. [16]).

2.2. Laser-induced ion mass analysis

This is a relatively new semiquantitative technique, but has the advantage of being able to analyse the light elements, which hitherto has proved difficult. In such instruments a short pulse of high-energy laser radiation is focused on to the specimen surface. This results in the evaporation and partial ionization of a few cubic micrometres of material. Analysis of the resulting ions is effected using a time-of-flight mass spectrometer (e.g. [17]).

2.3. Texture determination

Pole figures, derived from X-ray goniometric analysis taken with an X-ray camera, allow the quantification of texture (e.g. [18]).

Electron back scattering is a diffraction technique which can be effected in a scanning electron microscope and permits local orientation to be determined with a spatial resolution better than 1 μm (e.g. [19, 20]). By relating these local orientations to the crystal axes or the specimen axes, texture measurements can be collated on a grain-specific basis [21].

3. Results

3.1. Formation of grain banding

The solution heat treated and aged microstructure appeared to be partially recrystallized, both at the surface (Fig. 1a) and at the centre (Fig. 1b). The recrystallization was also seen to be anomolous. At the surface the grains were equiaxed, with a size ranging from 4 to 72 μm. At the centre many grains were pancake-shaped ranging from 8 to 44 μm wide, and 48 to 190 μm long. In both cases precipitates are clearly evident, which were lithium rich. The change in grain size occurred at 400 μm from each surface (the sheet thickness being 1600 μm).

3.2. Wavelength dispersive X-ray spectroscopy

Fig. 2a shows the WDS plot for copper and magnesium across the short transverse direction of the alloy sheet. The magnesium plot shows depletion at both surfaces, with a consistent composition throughout most of the sheet. The composition plot for copper, however, shows a steep increase in concentration 400 μm from the surface. This rises from a central region of even compositional concentration. Owing to this change in copper concentration, which occurred at approximately 400 μm from each surface, and which corresponds to the grain size change, it seemed apparent, all other things being equal, that the copper concentration was responsible for the changed grain morphology. However, a lithium profile was needed, but due to the lack of ability to detect the light elements by WDS, the lithium profile across the alloy sheet was measured using LIMA.

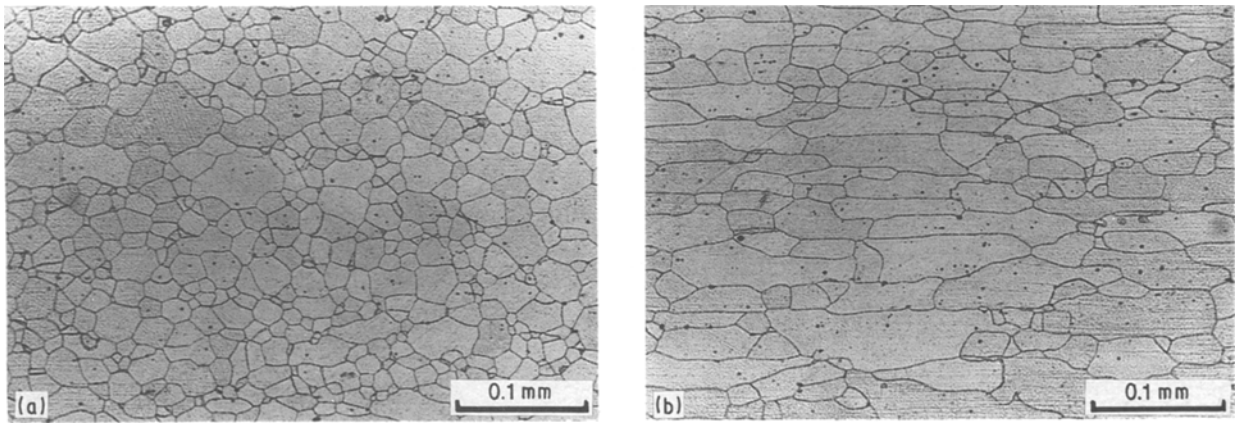

Figure 1 (a) Micrograph showing the reduced anomolous grain size and equiaxed shape of grains, at the surface of the alloy sheet. Precipitates are clearly evident which were found to be lithium rich. (b) Micrograph showing the anomolous recrystallization behaviour and resultant pancake-shaped grains at the centre of the alloy sheet, as viewed in the transverse direction. Again lithium-rich precipitates are clearly evident.

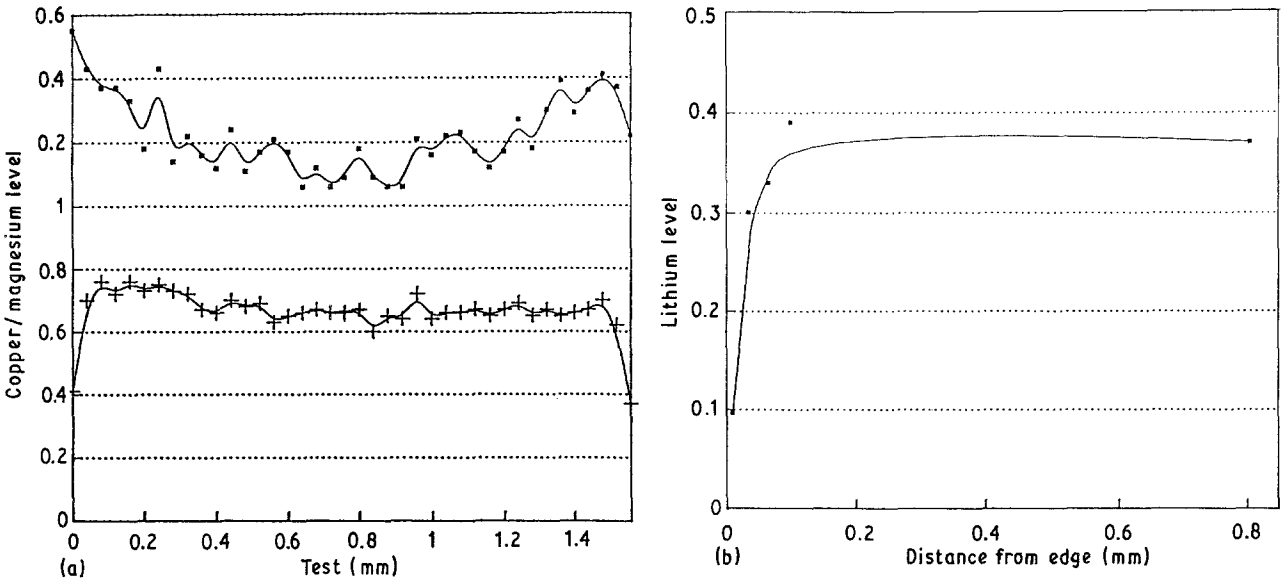

Figure 2 (a) Graph showing the compositional plot for (■) copper and (+) magnesium across a tranverse section of the alloy sheet. The magnesium plot shows a fairly consistent level across most of the alloy sheet with only a "tailing off" at the edges due to surface depletion. The copper concentration shows an increase outwards, from a depth of approximately 400 μm from both surfaces. This depth corresponds to a quarter of the thickness of the alloy sheet, and is the same depth at which the grain-size variation occurred, as in Figs 1a and b. (b) Graph showing the variation in (■) lithium content half-way across the same transverse section of the alloy sheet, as that which showed the grain size change and copper concentration variation. Here lithium's surface depletion is noted in the outer 100 μm, although no concentration change is noted at 400 μm from the surface, corresponding to the above copper and grain size change.

3.3. Laser-induced ion mass analysis

The lithium profile across the short transverse section of the alloy sheet by LIMA is shown in Fig. 2b. Here a steep increase is seen from each surface to a depth of approximately 100 μm. From this point the curve levels off showing a consistent concentration of lithium throughout most of the alloy sheet. This overall trace for lithium discounts any responsibility for the grain morphology change, which occurred at 400 μm from each surface, on lithium's behalf.

3.4. X-ray goniometric analysis

Figs 3a to c show the pole figures at 400, 530 and 800 μm from the surface, respectively. In each case the 2 0 0 and 1 1 1 pole figures are given. A purely elementary review of each pole figure shows a distinct change in texture between the grains at the surface compared to those in the central region of the alloy sheet. It therefore seemed quite apparent that not only was there a distinct grain size change, with an associated copper content variation, but also a distinct textural change, running from edge to centre through the thickness of the alloy sheet.

3.5. Electron back scattering

By use of this technique, confirmation of the textural change observed by standard X-ray goniometry was sought. Figs 4a and b are the pole figures representing these textural data. Here, too, a distinct change in texture is observed, when the data from grains from the centre and surfaces of the alloy sheet are compared. As with the X-ray pole figure results, the EBSP results are discussed in detail below.

4. Discussion

To recapitulate, an increase in the fracture toughness of our test alloy is desirable in that the larger the initial length for onset of fast fracture, the better the chance of detection prior to catastrophic failure.

The as-received alloy (in the T3 condition) was solution heat treated for 0.5 h at 540° C, water quenched, and aged for 16 h at 190° C. Figs 1a and b show the resultant microstructural appearance of grains at the centre and edge of the alloy sheet, respectively. This variation in the resultant microstructure between the surface and centre of the aluminium–lithium sheet occurred approximately 400 μm from each surface. Fig. 2a shows the composition plot for copper and magnesium across the alloy sheet. Here the magnesium level shows a uniform presence, except in the last 100 μm from the edge, where surface depletion is evident. The compositional plot for copper was intriguing, in that a reduction of copper towards the centre formed the basis of a U-shaped plot. If this plot is divided into three sections, the first from zero to 400 μm, the second from 400 to 1200 μm, and the third from 1200 to 1600 μm, the U-shaped plot shows three distinct areas. At the surfaces a drop in copper content is seen decreasing towards the centre with the central portion showing a uniform copper content. Computational analysis of the EBS data, showed a uniform percentage of 18% of low-angle or special grain boundaries at the centre and edge of the specimen; with the edge showing a more equiaxed grain structure, recrystallization here appeared to be complete. At the centre, however, the pancake-shaped grains gave rise to the speculation that recrystallization was only partial. The lithium variation across the alloy sheet was determined using LIMA. Fig. 2b shows the lithium profile across the alloy sheet. Here, a steep increase in the lithium content is shown in the first 100 μm from the

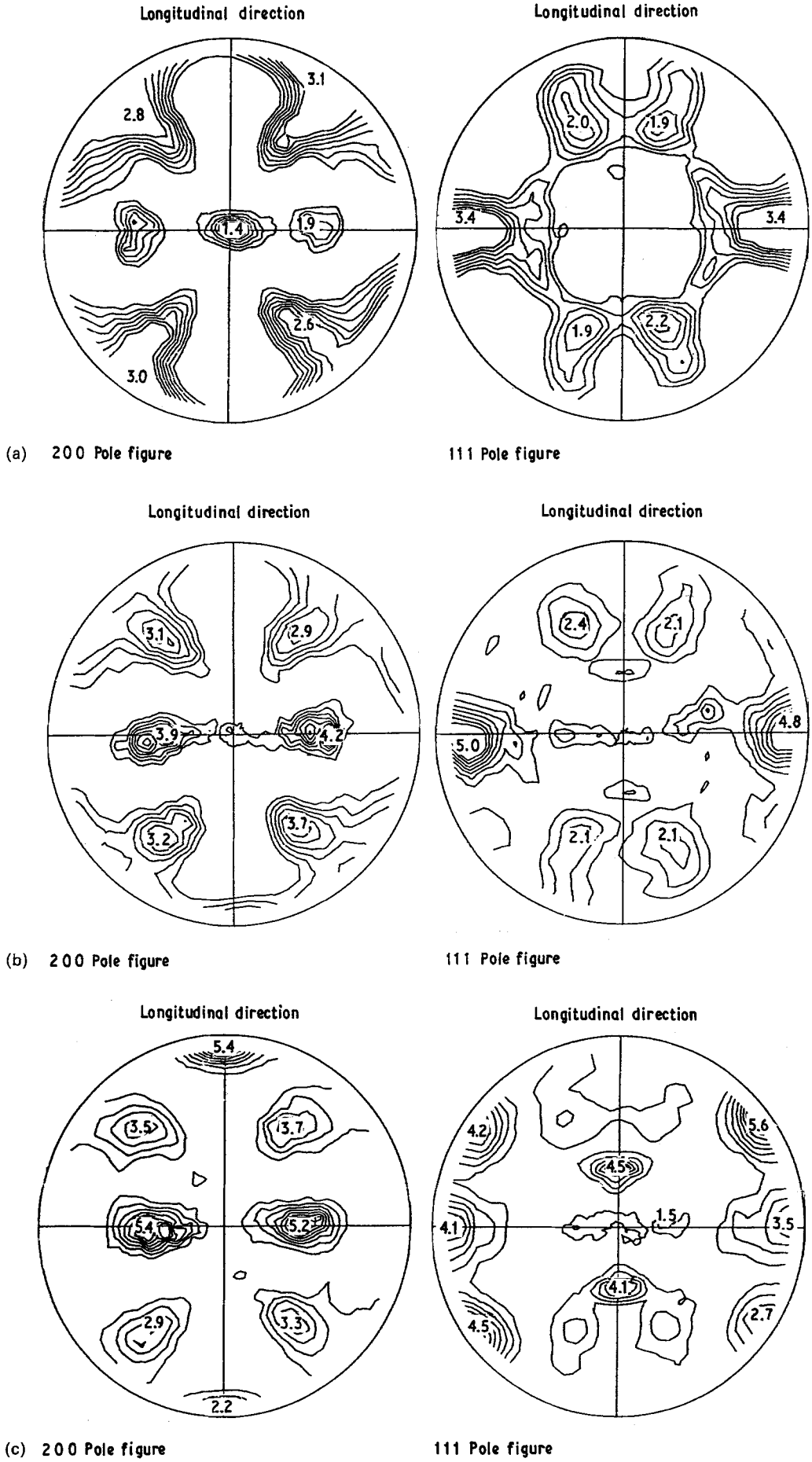

Figure 3 (a) 200 and 111 pole figures taken via goniometric analysis 400 μm from the surface of the alloy sheet. The normal direction of the 200 pole figure shows a strongish 001 with the transverse and rolling directions showing no 001 tendency. From the 111 pole figure it is clear that the (111)⟨111⟩ component has been eliminated. (b) Corresponding 200 and 111 pole figures, 530 μm from the surface. Here the 200 pole figure shows deviation from the strongish 001 around the normal direction, and the 111 pole figure shows a partial (111)⟨111⟩ component. (c) Corresponding 200 and 111 pole figures, 800 μm from the surface of the alloy sheet. No pole around the normal direction of the 200 pole figure indicates a lack of cube texture. A strong 001 type pole is evident in the rolling direction.

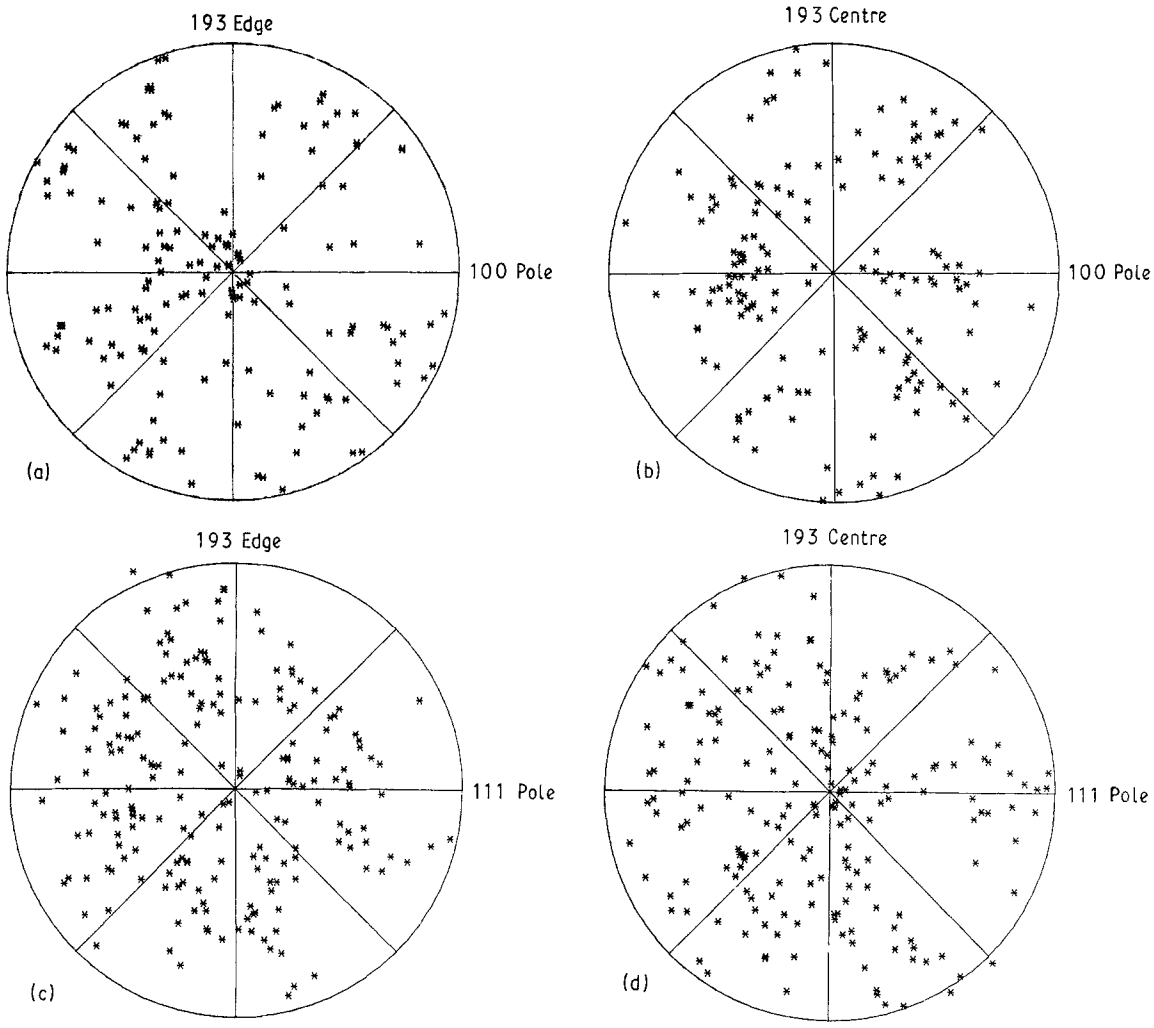

Figure 4 (a) 1 0 0 stereographic projection of data collected using the EBS technique, showing the textural illustration of a selection of 50 grains at the surface of the alloy sheet. Here a strong 1 0 0 type cube texture is clearly evident. (b) Corresponding textural illustration in stereographic form, of the EBSP data from the centre of the alloy sheet, showing a marked deviation from the cube texture noted in (a). (c) 1 1 1 stereographic projection of data collected using the EBS technique, showing the textural illustration of a selection of 50 grains at the surface of the alloy sheet. No strong textural bias can be deduced. (d) Corresponding textural illustration for the centre of the alloy sheet. Here a marked tendency towards a 1 1 1 rolling texture can be observed.

alloy's surface. At 100 μm from the surface, a much more gradual increase and levelling off is seen. The lithium content variation was, therefore, concluded to have no effect upon the resultant grain size change observed.

Following on from the microstructural analysis, a texture investigation of the alloy's surface and central grains was instigated. Figs 3a to c show the X-ray goniometric pole figures at 400, 530 and 800 μm from the surface, respectively. Each has been drawn for the 2 0 0 pole figure and the 1 1 1 pole figure. At 400 μm from the surface (Fig. 3a) the normal direction shows a relatively strong 0 0 1, but the transverse and rolling directions show no 0 0 1 tendency. The (1 1 1)$\langle$1 1 1$\rangle$ component has been eliminated. This is apparent when there is a strong cube texture, where the surface grains have been most affected by the recrystallization process. Fig. 3b shows the pole figure at 530 μm from the surface, where there is a tendency to move away from a recrystallized cube texture. Fig. 3c shows the pole figures at 800 μm from the surface, again derived by X-ray goniometry, where no pole around the normal direction is evident so that no cube texture is detected. Instead the pole figures show a strong 0 0 1 type in the rolling direction. These data showed a marked textural change between the surface and central grains of the alloy sheet with a recrystallized cube texture at the surface, and a rolling texture at the centre.

Figs 4a to d show the 1 0 0 and 1 1 1 stereographic projections of data collected using the EBS technique, for grains at the surface and centre of the alloy sheet, respectively. Fig. 4a shows a strong 1 0 0-type cube texture at the surface, whereas Fig. 4b shows a deviation from this cube texture for grains at the centre evident in Fig. 4d as a strong 1 1 1 rolling texture. These data confirm the previous data, and it is worth noting that the sample selection for the EBS system in this case is only 50. For the X-ray goniometry, a sample selection of 10 000 to 100 000 is common. This correlation is quite marked and establishes the integrity of the EBS system for textural analysis. Also the EBS technique has the ability to yield data on a grain specific basis, and therefore is able to yield misorientation data and information about the angle of rotation between contiguous grains.

As far as our test alloy was concerned therefore, not only was there a grain size change and copper content change at approximately 400 μm from the surface,

there was also a textural change. Our future study will concentrate on the thermomechanical treatment of the alloy, to try to ascertain the reasoning behind the recrystallization behaviour observed, as it can be safely concluded that, the grain-banding effect was not solely due to uneven elemental distributions. Transmission electron microscopy (TEM) work will also be required to establish the extent of recrystallization across the sheet by establishing the density of dislocations at the surface and centre. Examination of the copper distribution via TEM would similarly be advantageous.

5. Conclusions

1. There is a grain-size variation at approximately 400 μm from the surface. There is also a textural variation, seeming to imply that the effect is due to some function of the hot/cold thermomechanical treatment, and not simply an effect of the distribution of chemical species.

2. A distinct copper variation was observed across the sheet. The change in concentration appeared to correspond to the grain size variation shown previously.

3. The lithium analysis via LIMA showed that lithium was not responsible for the grain-size variation.

4. The magnesium trend showed no variation across most of the alloy sheet, with only a surface depletion in the outer 100 μm which had no influence upon the grain-size variation.

Acknowledgements

Financial support and supply of experimental material from the Ministry of Defence at RAE Farnborough is gratefully acknowledged by the authors. The use of LIMA at Cambridge was through the courtesy of Dr E. R. Wallach.

References

1. D. LITTLE, in "Aluminium Lithium Alloys III" edited by C. Baker *et al.* (Dotesios, Bradford-on-Avon, 1985) p. 15.
2. C. J. PEEL, D. McDARMAID and B. EVANS, "Westec", Los Angeles (1987) (ASM Int., Metals Park, Ohio) pp. 315–37.
3. B. EVANS, D. S. McDARMAID and C. J. PEEL, SAMPE Montreaux Conference (1984) Private communication.
4. C. J. PEEL and P. J. E. FORSYTH, *Met. Sci. J.* **7** (1973) 121.
5. E. GRANT, A. J. PORTER and B. RALPH, *J. Mater. Sci.* **19** (1984) 3354.
6. P. L. MAKIN, PhD dissertation, Cambridge University (1985).
7. W. S. MILLER, J. WHITE and D. J. LLOYD, *Engng Mater. Adv. Service* **3** (1986) 1799.
8. F. W. GAYLE and J. B. VANDERSANDE, in "Aluminium Lithium Alloys III" edited by C. Baker *et al.* (Dotesios, Bradford-on-Avon, 1985) p. 376.
9. H. M. FLOWER and P. J. GREGSON, *Mater. Sci. Technol.* **3** (1987) 81.
10. B. NOBLE and G. E. THOMPSON, *ibid.* **5** (1971) 114.
11. D. B. WILLIAMS and J. W. EDINGTON, *Met. Sci. J.* **9** (1975) 529.
12. J. M. SILCOCK, *J. Inst. Met.* **88** (1959–60) 357.
13. P. S. PAO, K. K. SANKAVAN and J. E. O'NEAL, in "Aluminium–Lithium Alloys III" edited by C. Baker *et al.* (Dotesios, Bradford-on-Avon, 1981) pp. 307–23.
14. M. FURUKAWA, Y. MIUVA and M. NEMOTO, HVEM Laboratory, Kyushu University. (1986) Annual Report No. 10.
15. I. J. POLMEAR, "Light Alloys" (Arnold, London, 1980) p. 22.
16. P. D. PITCHER, *Appl. Microscan 9 Microanalyser, RAE* (1981).
17. E. R. WALLACH and J. A. LEAKE, *Encyclopedia Mater. Sci. Engng* **1** (1988) 253.
18. E. GRANT, D. JUUL JENSEN, N. HANSEN, B. RALPH and W. M. STOBBS, in Proceedings Risø International Symposium on Annealing edited by N. Itansen *et al.* (Risø Press, Roskilde, Denmark, 1986) pp. 329–36.
19. K. BABA KISHI and D. J. DINGLEY, in "Proceedings XIth International Congress on Electron Microscopy", Kyoto (1986) edited by T. Imura *et al.* (Japanese Society of E.M., Tokyo, 1986) pp. 741–2.
20. J. HJIELEN, *ibid.* pp. 251–2.
21. V. RANDLE and B. RALPH, *Proc. R. Soc. Lond.* **A415** (1988) 239.

Received 19 May
and accepted 23 October 1989